AIP Journal of Applied Physics

Issues on the pulse-width dependence and the shape of acoustic radiation induced static displacement pulses in solids

Karthik Thimmavajjula Narasimha, Elankumaran Kannan, and Krishnan Balasubramaniam

Citation: Journal of Applied Physics **105**, 073506 (2009); doi: 10.1063/1.3093873
View online: http://dx.doi.org/10.1063/1.3093873
View Table of Contents: http://scitation.aip.org/content/aip/journal/jap/105/7?ver=pdfcov
Published by the AIP Publishing

Articles you may be interested in

Shape profile of acoustic radiation-induced static displacement pulses in solids
J. Appl. Phys. **108**, 013512 (2010); 10.1063/1.3457850

Temporal analysis of tissue displacement induced by a transient ultrasound radiation force
J. Acoust. Soc. Am. **118**, 2829 (2005); 10.1121/1.2062527

Simulation of ultrasonic pulse propagation, distortion, and attenuation in the human chest wall
J. Acoust. Soc. Am. **106**, 3665 (1999); 10.1121/1.428209

The effect of abdominal wall morphology on ultrasonic pulse distortion. Part II. Simulations
J. Acoust. Soc. Am. **104**, 3651 (1998); 10.1121/1.423947

Erratum: “Simulation of ultrasonic pulse propagation through the abdominal wall” [J. Acoust. Soc. Am. 102, 1177–1190 (1997)]
J. Acoust. Soc. Am. **104**, 1124 (1998); 10.1121/1.423361

[This article is copyrighted as indicated in the article. Reuse of AIP content is subject to the terms at: http://scitation.aip.org/termsconditions. Downloaded to] IP: 134.129.164.186 On: Sat, 20 Dec 2014 17:21:28

Issues on the pulse-width dependence and the shape of acoustic radiation induced static displacement pulses in solids

Karthik Thimmavajjula Narasimha, Elankumaran Kannan,[a] and Krishnan Balasubramaniam[b]
Department of Mechanical Engineering and Center for Nondestructive Evaluation, Indian Institute of Technology Madras, Chennai 600036, India

(Received 30 July 2008; accepted 2 February 2009; published online 3 April 2009)

Recent experimental results showing the pulse width independence and the flat topped shape of static displacement generated during finite amplitude sinusoidal ultrasonic tone burst propagation in solids and the contradicting previous results reported in the literature are considered. The pulse width independence is analytically confirmed and the flat topped shape is explained by considering the progressive spatial and time domain shapes of the static strain and displacement pulses. A numerical simulation of the finite amplitude longitudinal ultrasonic wave propagation in solids has been performed to further verify the pulse width independence of the static displacement pulse.
© *2009 American Institute of Physics*. [DOI: 10.1063/1.3093873]

I. INTRODUCTION

The field of nonlinear ultrasonics, which uses finite amplitude sinusoidal ultrasonic tone burst propagation in solids, has been witnessing an increased attention over the past few decades owing to its ability to discern microstructural features.[1–6] On the time scale of microseconds, which is the typical order of the width of the tone bursts used in this case, lattice anharmonicity, dislocations, and various dislocation arrangements are responsible for the nonlinearities in the material, the distortion of the wave and consequent generation of the higher order harmonics, and the static displacement. In general, nonlinear ultrasonics relies on measuring the nonlinearity parameter evaluated from the generated second harmonic during the finite amplitude longitudinal propagation of an ultrasonic tone burst in solids.[6] Although nonlinearity parameter can be measured using the conventional harmonic generation technique, measuring it using static displacement generation experiments[7] offers the advantage of being cost effective by cutting down on the receiver side instrumentation. Further the nonlinearity parameter can be measured in the time domain as against frequency domain measurements in harmonic generation experiments.[7] It can be seen that recently considerable attention is being devoted in measuring the static displacement to utilize this technique to measure nonlinearity parameter.[7–9]

The phenomenon of the static displacement generation in solids during the finite amplitude sinusoidal ultrasonic wave propagation was originally studied by Thurston and Shapiro[10] and later explored theoretically by Cantrell[11] and experimentally by Yost and Cantrell.[12] Cantrell's[11] analytical treatment of the generation of the static displacement predicts that it varies as the square of the input amplitude, frequency of the wave, and linearly with the material nonlinearity parameter and also the width of the tone burst. These predictions have been verified experimentally by Yost and Cantrell.[12] Further, they analytically derived and verified experimentally that the shape of the static displacement pulse as received on the receiver side is a right triangle in the time domain. However, the tone burst dependence of the static displacement and the shape of the static displacement pulse as reported by Yost and Cantrell[12] were recently refuted by Jacob *et al.*[8] based on their experimental observations. Their systematic experiments reveal that the right triangular shape of the static displacement observed by Yost and Cantrell[12] could be due to the low pass filter used in the receiver instrumentation to extract the static displacement. They have also shown that by choosing an appropriate low pass filter, one can extract the true static displacement that depends on the distance of propagation rather than on the width of the tone burst and is flat topped in shape. Very recently, Cantrell[9] explained the results of Jacob *et al.*[8] by suggesting that the diffraction effects due to the laser spot size in the detection system of Jacob *et al.*,[8] attenuation in polycrystalline material used by them and dispersive nature of the medium could have caused the static displacement to be of rectangular (flat topped) shape in their experiments. Cantrell[9] asserted that although the static displacement pulse reaches the receiver end as a right triangular pulse, the detection system used could make it a rectangular (flat topped) pulse. Since the effects of attenuation, dispersion, and diffraction were absent in the experiments of Yost and Cantrell,[12] Cantrell asserted that they could extract the static displacement as predicted by the model of Cantrell[11] and Yost and Cantrell.[12]

However our research in this aspect proves that even for such a medium such as silicon, which is nonattenuating and is nondispersive, the static displacement reaches the receiver end as a flat topped signal and not as a right triangular signal in the time domain and is independent of the width of the tone burst. The present article is concerned with the analytical proof of the same. To independently prove the point of pulse width independence of the static displacement pulses, numerical simulations have been carried out using finite dif-

[a]Presently at RKM Vivekananda College, Chennai-600 004, India.
[b]Author to whom correspondence should be addressed. Electronic mail: balas@iitm.ac.in.

 © 2009 American Institute of Physics

[This article is copyrighted as indicated in the article. Reuse of AIP content is subject to the terms at: http://scitation.aip.org/termsconditions. Downloaded to] IP: 134.129.164.186 On: Sat, 20 Dec 2014 17:21:28

ference time domain approach which simulates the propagation of the wave in the solid and does not include any effects of wave dispersion, attenuation, and diffraction in the detection system.

II. ANALYTICAL FORMULATION

In the one dimensional form, the equation governing the propagation of the finite amplitude ultrasonic wave in a solid is given by

$$\rho\frac{\partial^2 u}{\partial t^2} = E\frac{\partial^2 u}{\partial x^2}\left(1 - \beta\frac{\partial u}{\partial x}\right). \tag{1}$$

Following the particle velocity solution, Yost and Cantrell[12] solved the above equation to derive the expression for the generated static strain. Their analytical formulation asserts that the wave propagation results in the propagation of a flat topped strain pulse within the spatial extent of the wave and is given by

$$\left\langle\frac{\partial u}{\partial x}\right\rangle = \frac{1}{8}\beta k^2 (u_0)^2. \tag{2}$$

Integrating the above equation with respect to the spatial coordinate, Yost and Cantrell[12] showed that the output static displacement pulse would be in the shape of a right triangle. They further suggested that as the static displacement pulse approaches the receiving end of the sample, the maximum displacement amplitude of the pulse arrives first. This would result in a mirror image of the static displacement waveform, as given in Fig. 2 in the work of Yost and Cantrell.[12] Further, they reported that the measured static displacement pulse on the receiver end using a capacitive detector-low pass filter arrangement was right triangular in shape whose peak amplitude varies linearly with the pulse width of the tone burst.

Yost and Cantrell[12] and Cantrell[9] suggested that the static displacement pulse grows in magnitude over the spatial extent of the tone burst where the energy (E) is nonzero and hence is dependent only on the width of the tone burst and not on the distance of propagation. While the static displacement grows in magnitude only over the spatial extent of the wave where $E \neq 0$, the fact that has been ignored in their derivations is that the trailing end of the wave has a nonzero static displacement value once the static displacement pulse leaves the transmitter and consequently the leading edge would grow in magnitude. By taking into account the static displacement at the trailing end of the wave to the integration carried out with respect to the spatial domain in Eq. (2), one can find that the static displacement depends on the distance of propagation. The derivations are presented in the following.

Let us assume that l is the spatial extent of the tone burst and that the wave is currently confined to the region $x_0 \leq x \leq x_0 + l$ for some x_0. Following the formula for the equation of a straight line, $y(x) = y(x_0) + \int_{x_0}^{x} (\text{slope}) dx$ [where $y(x)$ is the ordinate at abscissa x and slope is the slope of the straight line].

The static displacement, $dc(x)$, for $x_0 \leq x \leq x_0 + l$ can be evaluated as

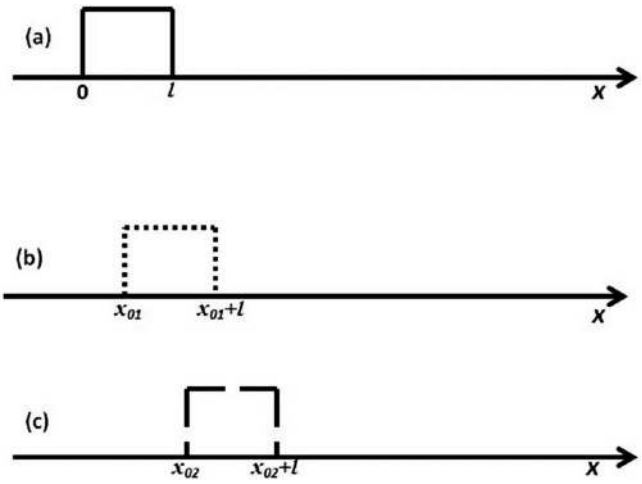

FIG. 1. The static strain pulse in the spatial domain at three different instants of time.

$$dc(x) = dc(x_0) + \int_{x_0}^{x} \left\langle\frac{\partial u}{\partial x}\right\rangle dx. \tag{3}$$

It needs to be noted that $dc(x)$ is the value of the static displacement to be taken in the time interval $t_0 \leq t \leq t_0 + t_{pw}$ (where t_{pw} is the width of the tone burst and t_0 is the instant of time when the pulse arrives at the location x) in which it is defined, i.e., essentially over nonzero values of the energy (E) as suggested by Cantrell.[9] For $t \notin [t_0, t_0 + t_{pw}]$, $dc(x) \equiv 0$.

Let us consider the three cases, as shown in Fig. 1, with $0 \leq x_{01} \leq l$ and $x_{01} \leq x_{02} \leq x_{01} + l$. It will now be shown that the static displacement for $x \in [0, l]$, $x \in [x_{01}, x_{01} + l]$, and $x \in [x_{02}, x_{02} + l]$ is given by

$$dc(x) = \tfrac{1}{8}\beta k^2 (P_j)_0^2 x. \tag{4}$$

Case I. Initially consider the case when the strain pulse is as shown in Fig. 1(a). In this case, $x_0 = 0$ and $dc(0) = 0$ (under the condition of a pure input sinusoidal wave with no static displacement) and hence

$$dc(x) = \int_0^x \left\langle\frac{\partial u}{\partial x}\right\rangle dx = \frac{1}{8}\beta k^2 (P_j)_0^2 x \quad \text{for} \quad 0 \leq x \leq l. \tag{5}$$

Further it needs to be noted that since the strain is constant over the spatial $(0 \leq x \leq l)$ and time domains (since it propagates as a flat topped pulse), $dc(x)$ for $t \in [t_0, t_0 + t_{pw}]$ would not have any time dependence as none of the right hand side quantities has a time dependence in Eq. (5). Thus, for each $x \in [0, l]$, the above equation holds for all $t \in [t_0, t_0 + t_{pw}]$, where t_0 is the time when the wave reaches the location x.

Case II. Consider the case when the strain pulse is as shown in Fig. 1(b).

Now $dc(x)$ for this case is given by

[This article is copyrighted as indicated in the article. Reuse of AIP content is subject to the terms at: http://scitation.aip.org/termsconditions. Downloaded to] IP: 134.129.164.186 On: Sat, 20 Dec 2014 17:21:28

$$dc(x) = dc(x_{01}) + \int_{x_{01}}^{x} \left\langle \frac{\partial u}{\partial x} \right\rangle dx = \frac{1}{8}\beta k^2 (P_j)_0^2 x_{01} + \frac{1}{8}\beta k^2 (P_j)_0^2 (x - x_{01}),$$

wherein we have used that since $x_{01} \in [0, l]$ and since the wave has not left the point at $x = x_{01}$ yet; from Case I, $dc(x_{01}) = 1/8\beta k^2 (P_j)_0^2 x_{01}$.

Hence, in this case also, it can be concluded that $dc(x) = 1/8\beta k^2 (P_j)_0^2 x$.

Case III. Now consider the case shown in Fig. 1(c). In this case, we can write

$$dc(x) = dc(x_{02}) + \int_{x_{02}}^{x} \left\langle \frac{\partial u}{\partial x} \right\rangle dx = \frac{1}{8}\beta k^2 (P_j)_0^2 x_{02} + \frac{1}{8}\beta k^2 (P_j)_0^2 (x - x_{02}).$$

Here we used that from Case II, since $x_{02} \in [x_{01}, x_{01} + l]$, $dc(x_{02}) = 1/8\beta k^2 (P_j)_0^2 x_{02}$. Hence even for this case we conclude that $dc(x) = 1/8\beta k^2 (P_j)_0^2 x$.

It should be noted that the choices of x_{01} and x_{02} is arbitrary with the only constraint that the domains $[0, l]$ and $[x_{01}, x_{01} + l]$ should have at least one point in common where the static strain is nonzero (that is the nonzero part of the strain curves at two instants of time overlapping) with a similar constraint for the domains $[x_{01}, x_{01} + l]$ and $[x_{02}, x_{02} + l]$. Since we chose three instances at which the strain pulses are as shown, the above derivation is valid $\forall 0 \le x \le 3l$. As a simple extension, by choosing a finite number of such domains, we can extend the above derivation and show that $dc(x) = 1/8\beta k^2 (P_j)_0^2 x \, \forall x$.

Thus we see that although as argued by Cantrell,[9] the static displacement grows only in the region where $E \neq 0$ and is zero elsewhere, due to the fact that the static displacement at the trailing end is nonzero. Once the wave leaves the transmitter the static displacement at the leading edge grows with the distance of propagation.

III. ON THE SPATIAL AND TIME DOMAIN SHAPES OF THE STATIC STRAIN AND DISPLACEMENT PULSES

Yost and Cantrell[12] and Cantrell[9] suggested that the shape of the static displacement pulse is a right triangle. It needs to be noted that this is in the spatial domain. From the above derivations, it is clear that when the spatial extent of the wave is lesser than the length of the sample (as is the case with all usual nonlinear ultrasonic experiments), the shape of static displacement pulse in the spatial domain is a right angled triangle until the trailing end of the wave leaves the transmitter and is trapezium once it leaves the transmitter. As the static displacement pulse reaches the receiver end, it is recorded in the time domain at the receiver by the detection system. In the following, the shape of the static displacement pulse in the time domain received at the receiver is discussed.

Consider the static displacement pulse at any given instant when the wave is in the region $x_0 \le x \le x_{01} + l$. The static displacement is in the shape of a trapezium. as shown in Fig. 2(a). To determine the shape of the transmitted static displacement pulse as received at the receiver side, consider three representative points a, b, and c on the pulse in the spatial domain, as shown in Fig. 2(a). Assuming that we receive the pulse at position a (i.e., a is the receiving end of the sample), the displacement value recorded initially will be y_1. The displacement at b will be received at a at a later time (say, t_1). In light of the previous discussion, it is clear that by the time this displacement at b reaches a, it increases in value to y_1 and is received as y_1. Same is the case with the displacement at point c as received at a at a later time (say, t_2). Thus although the signal is in the form of a trapezoid in the spatial domain, it is received as a flat topped signal in the time domain, as shown in Fig. 2(b). It can be concluded that although static displacement pulse is not flat topped in the spatial domain, it is received as a flat topped pulse at the receiver end in the time domain. Thus, it appears that the triangular time domain pulses observed by Yost and Cantrell[12] were due to the filter characteristics interfering with the measurement as suggested by the experimental results of Jacob *et al.*[8]

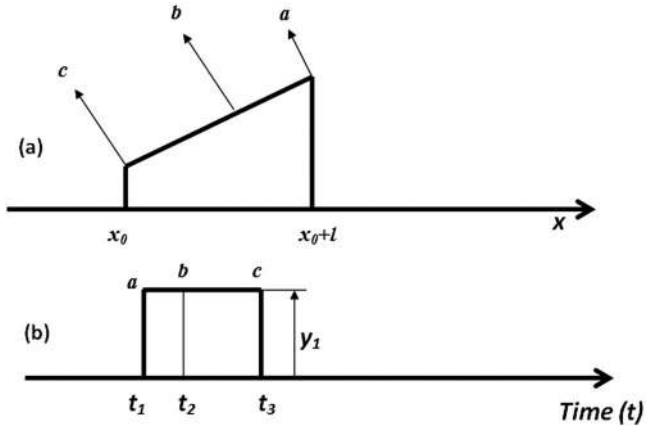

FIG. 2. (a) The static displacement pulse in the spatial domain. (b) The displacement pulse in the time domain as received at the receiver.

IV. STATIC DISPLACEMENT FROM FINITE DIFFERENCE TIME DOMAIN SIMULATION

To further test the point of pulse width independence of the static displacement, nonlinear wave propagation in a solid when the effects of dispersion and attenuation can be neglected is numerically simulated using a finite difference time domain approach.

The discretized equation corresponding to the governing equation (1) using $\partial u/\partial x = (u_{i+1}^t - u_{i-1}^t)/2\Delta x$ and $\partial^2 u/\partial x^2 = (u_{i+1}^t - 2u_i^t + u_{i-1}^t)/(\Delta x)$ is

$$u_i^{t+\Delta t} = 2u_i^t - u_i^{t-\Delta t} \frac{(\Delta t)^2}{\rho (\Delta x)^2} \left[E(u_{i+1}^t - 2u_i^t + u_{i-1}^t) - \frac{E\beta}{2\Delta x}(u_{i+1}^t - 2u_i^t + u_{i-1}^t)(u_{i+1}^t - u_{i-1}^t) \right], \quad (6)$$

where u_i^t is the displacement at time t at the ith node, where ρ is the density of the material, A is its area of cross section, Δt and Δx are the time step and distance between two con-

[This article is copyrighted as indicated in the article. Reuse of AIP content is subject to the terms at: http://scitation.aip.org/termsconditions. Downloaded to] IP: 134.129.164.186 On: Sat, 20 Dec 2014 17:21:28

TABLE I. Validating the numerical simulations using second harmonic generation (columns 2 and 3) and theory of generation of static strain pulses (columns 4 and 5).

Distance of propagation (mm)	Second harmonic from simulations (pm)	Second harmonic (analytical solution) (pm)	Static strain in picostrains (from simulations)	Static strain in picostrains (Cantrell's theory)
2.5	1.0173	0.90402	367.05	361.61
5	1.9523	1.808	366.94	361.61
7.5	2.8612	2.7121	367.1	361.61
10	3.772	3.6161	367.12	361.61
12.5	4.6969	4.5201	367.03	361.61
15	5.6146	5.4241	366.88	361.61
17.5	6.5402	6.3281	366.68	361.61
20	7.4639	7.2321	366.48	361.61
22.5	8.3805	8.1362	367.24	361.61
25	9.2987	9.0402	367.32	361.61
27.5	10.21	9.9442	367.46	361.61
30	11.124	10.848	367.51	361.61

secutive nodes in the discretization scheme, respectively, and E and β are the second order elastic constant and the nonlinearity parameter of the material, respectively. The boundary condition u_1^t is evaluated using the sinusoidal tone burst equation

$$u_1^t = A\ \sin(\omega t) \quad \text{for} \quad t \in [0, nt_0] = 0 \quad \text{otherwise}, \tag{7}$$

where t_0 is the time period, A is the input amplitude, ω is the frequency, and n is the number of cycles in the tone burst. A computer code has been written to carry out these simulations.

To validate the simulations, they were verified for the magnitude of the generated second harmonic. Following the analytical solution for the second harmonic by Hikata *et al.*,[13] the second harmonic obtained by taking the fast Fourier transform of the displacement profiles from simulation results were compared with the analytical solution for various values of the input parameters (input amplitude, frequency, nonlinearity parameter, and distance of propagation). The numerical and analytical values are found to be in close agreement. Table I (columns 2 and 3) show a typical comparison of the same.

The static strain values from the simulations were evaluated from the fast Fourier transform of the simulated strain profiles. These values were compared with the ones obtained using Yost and Cantrell's[12] equation for the static strain by plugging in the values of the input parameters in the right hand side of the Eq. (2). The simulated values and the analytical values are in close agreement within about 2% error, thus suggesting the fact that simulations are in excellent agreement with the strain pulse equations derived by Cantrell.[11] A typical comparison is shown in Table I (columns 4 and 5).

However, the results are different when we consider the static displacement. Once above discussed validations were done, the simulations were then carried out for different widths of the pulse width of the tone burst. The generated static displacement values for different pulse widths of the tone burst were compared for various values of the input parameters. A typical comparison for various distances of propagation is shown in Table II. It can be seen that the generated static displacement values are independent of the width of the tone burst. Figure 3 shows the plot of the generated static displacement with the distance of propagation for $\beta = 30$, $A = 10$ nm, $f = 0.796$ MHz, $E = 70$ GPa, and density of the material $(\rho) = 2700$ kg/m^3. It can be seen from the figure that the static displacement generated varies linearly with the distance of propagation. This has been verified for various values of the input parameters.

Therefore, we find that the numerical simulation of the finite amplitude ultrasonic tone burst propagation in solids also suggests the pulse width independence of static displacement. This is in accordance with the experimental evidence by Jacob *et al.*[8] and the analytical model proposed in this article. Our simulation results are an additional proof for the pulse width independence of the static displacement. The analytical model presented in this article and the numerical simulations further suggest that the results of Yost and Cantrell[12] could be due to the filter characteristics interfering with the measurement as suggested by Jacob *et al.*[8]

TABLE II. Invariance of the static displacement with the burst width of the tone burst (represented as number of cycles) and comparison with the theoretical model presented in this article.

Distance of propagation (mm)	Static displacement from theory (pm)	Static displacement (12 cycles) (pm)	Static displacement (16 cycles) (pm)	Static displacement (20 cycles) (pm)	Static displacement (24 cycles) (pm)
2.5	0.90402	1.0065	0.94767	0.92755	0.91887
5	1.808	1.6186	1.7345	1.7744	1.7916
7.5	2.7121	2.5992	2.6623	2.692	2.7049
10	3.6161	3.5576	3.6001	3.6147	3.621
12.5	4.5201	4.4935	4.5192	4.528	4.5318

[This article is copyrighted as indicated in the article. Reuse of AIP content is subject to the terms at: http://scitation.aip.org/termsconditions. Downloaded to] IP: 134.129.164.186 On: Sat, 20 Dec 2014 17:21:28

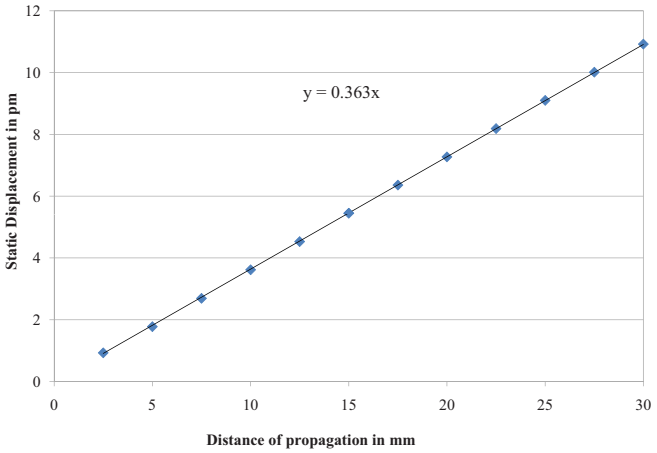

FIG. 3. (Color online) Variation in the static displacement with the distance of propagation for $f=0.796$ MHz, $\beta=30$, $A=10$ nm, $E=70$ GPa, and density of the material $(\rho)=2700$ kg/m^3.

V. CONCLUSIONS

Contradictions between the experimentally observed results of Jacob *et al.*[8] and Yost and Cantrell,[12] and the theoretical formulation in vogue to explain the static displacement generation in solids have been considered. Although Cantrell[9] suggested that dispersion, attenuation in polycrystalline material, and diffraction in the interferometric detection system, used by Jacob *et al.*,[8] could have caused the right triangular static displacement pulses to appear as rectangular, the present work analytically proves that even when these effects are negligible as in the case of Yost and Cantrell's[12] experiments on silicon using a capacitive detector, the static displacement pulse would be flat topped and independent of the width of the tone burst. A numerical simulation of the finite amplitude wave propagation in solids has been performed to further prove these points. The results from the present simulation studies further demonstrate that the static displacement generated depends directly on the distance of propagation rather than the width of the tone burst.

[1]P. B. Nagy, Ultrasonics **36**, 375 (1998).
[2]J. Frouin, S. Sathish, T. E. Matikas, and J. K. Na, J. Mater. Res. **14**, 1295 (1999).
[3]J. H. Cantrell and W. T. Yost, Int. J. Fatigue **23**, 487 (2001).
[4]D. J. Barnard, Appl. Phys. Lett. **74**, 2447 (1999).
[5]A. Wegner, A. Koka, K. Jenser, U. Netzelmann, S. Hirsekorn, and W. Arnold, Ultrasonics **38**, 316 (2000).
[6]C. Bermes, J. Y. Kim, J. Qu, and L. J. Jacobs, Appl. Phys. Lett. **90**, 021901 (2007).
[7]K. Thimmavajjula Narasimha, E. Kannan, and K. Balasubramaniam, Appl. Phys. Lett. **91**, 134103 (2007).
[8]X. Jacob, R. Takatsu, C. Barrière, and D. Royer, Appl. Phys. Lett. **88**, 134111 (2006).
[9]J. H. Cantrell, Appl. Phys. Lett. **92**, 231914 (2008).
[10]R. N. Thurston and M. J. Shapiro, J. Acoust. Soc. Am. **41**, 1112 (1967).
[11]J. H. Cantrell, Phys. Rev. B **30**, 3214 (1984).
[12]W. T. Yost and J. H. Cantrell, Phys. Rev. B **30**, 3221 (1984).
[13]A. Hikata, B. Chick, and C. Elbaum, J. Appl. Phys. **36**, 229 (1965).

[This article is copyrighted as indicated in the article. Reuse of AIP content is subject to the terms at: http://scitation.aip.org/termsconditions. Downloaded to] IP: 134.129.164.186 On: Sat, 20 Dec 2014 17:21:28